VOLUME 30, NUMBER 5, MAY 2015

ELSEVIER

THE JOURNAL OF ARTHROPLASTY

SELECTED KEY ARTICLES:

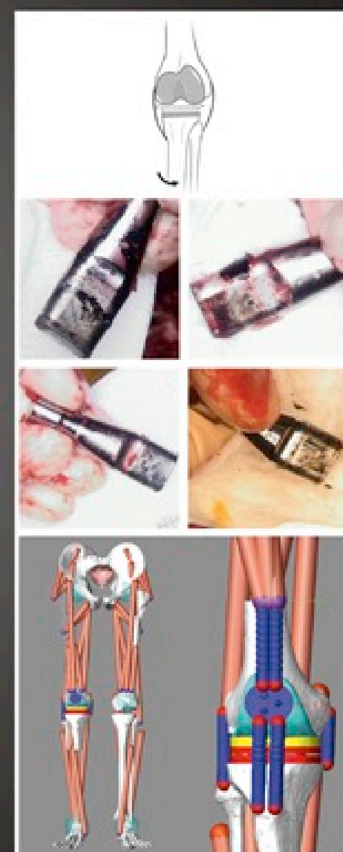

AAHKS
AMERICAN ASSOCIATION OF HIP AND KNEE SURGEONS

The Journal of Arthroplasty 30 (2015) 870–874

Contents lists available at ScienceDirect

The Journal of Arthroplasty

journal homepage: www.arthroplastyjournal.org

Patient-Specific Computer Model of Dynamic Squatting After Total Knee Arthroplasty

Hideki Mizu-uchi, MD, PhD [a,b], Clifford W. Colwell Jr., MD [a], Cesar Flores-Hernandez, BS [a], Benjamin J. Fregly, PhD [d], Shuichi Matsuda, MD, PhD [c], Darryl D. D'Lima, MD, PhD [a]

[a] *Shiley Center for Orthopaedic Research and Education at Scripps Clinic, Scripps Health, La Jolla, California*
[b] *Department of Orthopaedic Surgery, Graduate School of Medical Sciences, Kyushu University, Fukuoka, Japan*
[c] *Department of Orthopaedic Surgery, Graduate School of Medical Sciences, Kyoto University, Kyoto, Japan*
[d] *Department of Mechanical & Aerospace Engineering, University of Florida, Gainesville, Florida*

ARTICLE INFO

Article history:
Received 30 September 2014
Accepted 29 December 2014

Keywords:
total knee arthroplasty
squatting
computer model
knee contact force
patient-specific

ABSTRACT

Knee forces are highly relevant to performance after total knee arthroplasty especially during high flexion activities such as squatting. We constructed subject-specific models of two patients implanted with instrumented knee prostheses that measured knee forces in vivo. In vivo peak forces ranged from 2.2 to 2.3 times bodyweight but peaked at different flexion angles based on the type of squatting activity. Our model predicted tibiofemoral contact force with reasonable accuracy in both subjects. This model can be a very useful tool to predict the effect of surgical techniques and component alignment on contact forces. In addition, this model could be used for implant design development, to enhance knee function, to predict forces generated during other activities, and for predicting clinical outcomes.

Total knee arthroplasty (TKA) has become one of the most successful orthopedic procedures in providing pain relief and improving knee function, with reported survival rates of greater than 90% after 15 years [1,2]. The success of TKA is dependent on many factors including preoperative status, surgical technique, and the design and materials of the components. While survival rates are high, functional outcomes that facilitate common activities involving deep knee flexion such as kneeling, squatting, and sitting cross-legged are rarely achieved [3,4]. Knee contact force during activities after TKA is very important since it affects component wear and implant loosening. Knee contact force is related directly to the transmission of stresses through the implant, which include contact stresses generated at the bearing surface and subsurface, stresses at the implant–cement–bone interface, and stresses transmitted to underlying bone [5].

Previous studies have measured knee contact forces in cadaver models and biomechanical simulators. However, there are technical challenges in applying high physiologic loads to the knee joint coupled with the inherent weaknesses of extrapolating in vitro results to vivo function. While several computational models have predicted knee contact force, these reports vary widely based on the modeling approach and the assumptions inherent to the model. Predictions of tibiofemoral forces made by computer models have also varied widely for the same activity [6–9]. For example, peak forces predicted for walking prior to the availability of in vivo data ranged from 1.8 × BW to 8.1 × BW (times of bodyweight, reviewed by [10]). Peak forces predicted by computer models for squatting have also been variable, ranging from 3.4 × BW to 7.3 × BW [11–13].

The complexity of modeling the knee is in part due to tricompartmental contact with joint stability governed primarily by soft tissues. Knee contact forces can vary widely among patients due to differences in subject anatomy, bodyweight, and kinematic patterns. For accuracy, clinically relevant predictions and a subject-specific approach may be necessary to account for this interpatient variability. Subject-specific approaches have been reported with some validation of knee forces predicted during walking [10]. However, during weight-bearing deep knee bend activities such as squatting, the knee forces of the computer-generated model were much higher and until very recently these predictions had not yet been validated in vivo [11–14]. One recent study validated a subject-specific model of squatting with in vivo measured experimental knee forces and EMG [15]. The purpose of this study was to extend that approach by constructing subject-specific computer models of two different patients implanted with instrumented knee arthroplasty components, each performing two variations of a dynamic closed-kinetic-chain squatting activity. Patient kinematics and ground reaction forces were input into the model and the predicted tibiofemoral contact forces were compared to in vivo measured forces.

One or more of the authors of this paper have disclosed potential or pertinent conflicts of interest, which may include receipt of payment, either direct or indirect, institutional support, or association with an entity in the biomedical field which may be perceived to have potential conflict of interest with this work. For full disclosure statements refer to http://dx.doi.org/10.1016/j.arth.2014.12.021.

Reprint requests: Darryl D. D'Lima, MD, PhD, Shiley Center for Orthopaedic Research and Education at Scripps Clinic, Scripps Health, 11025 N. Torrey Pines Road, Suite 200, La Jolla, CA 92037, USA.

http://dx.doi.org/10.1016/j.arth.2014.12.021
0883-5403/

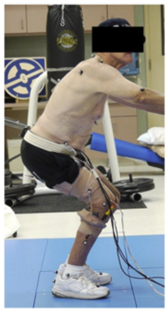

Fig. 1. Photograph of patient performing squatting motion.

Methods

Patient Information

Institutional review board approval and informed patient consents were obtained for this study. Three patients had been implanted with a custom tibial prosthesis instrumented with force transducers and a telemetry system [5,10,16–23]. The tibial prosthesis was customized to house force sensors and a telemetry system. The sensors measured three components of force and three components of moment acting on the tibial tray. These six measurements can be used to calculate the contact forces in the medial and lateral compartment. Two male patients were selected for this study (83-year-old, 69.5 kg, right knee; 88-year-old, 76.3 kg, left knee). One patient had no significant arthritis in his contralateral knee. The other patient had the contralateral knee replaced with the same design but without the custom tibia with electronics. Details of the implant design and surgical technique have been previously reported [18,24]. The distal femoral cut was made at a nominal 6° valgus to the anatomic axis of the femur using intramedullary alignment, while the posterior femoral cut was made in 3° external rotation with reference to the posterior condyles. The tibial bone cut was made at a nominal 90° to the long axis without any posterior slope. Standard cruciate-retaining Natural Knee® II (Zimmer) femoral components were cemented. The custom instrumented tibial prosthesis was cemented, and a 10 mm thick cruciate-retaining polyethylene insert was implanted. Measurements were made on postoperative computerized tomographic scans to obtain subject-specific femoral and tibial component alignment.

Experimental Measurement of Knee Forces In Vivo

The patients were three years postoperative at the time this study was conducted. Two different squatting activities were performed with both feet parallel to each other. For the first squatting activity patients were instructed to squat to the maximum knee flexion angle within tolerance and with the trunk flexed to a patient-preferred degree. For the second squatting activity, the patients were instructed to keep their hands on their hips and their upper body as upright as possible within tolerance (to minimize trunk flexion and maximize knee flexion moment). These variations were chosen to alter the external flexion moment on the knee. Each squatting cycle was repeated three times. Skin marker-based video motion analysis was used to record knee kinematics, and axial ground reaction forces were measured under each foot (Fig. 1).

Patient-specific Computer Model

Preoperative and postoperative computer tomographic scans were reconstructed to extract tibiofemoral bone geometry using MIMICS (Materialise, Leuven, Belgium). Computer-aided design models of the components were directly aligned to the 3-dimensional bone models as we have previously reported (Fig. 2) [25]. Bone and implant geometry was imported into a dynamic, musculoskeletal modeling program (LifeMOD/BodySIM 2008, LifeModeler, Inc., San Clemente, California). We previously validated a LifeMOD/KneeSim model using cadaver data measured in an Oxford knee rig [26]. A 14-segment model (head, trunk, upper arms, forearms, hands, thighs, legs, and feet) was initially constructed based on published generic anthropometric data (age, gender, bodyweight, and height) [27]. The body segments were then scaled, using measurements obtained from each patient. Each lower limb was then populated with 17 base muscles (gluteus maximus [2], gluteus medius [2], psoas major, iliopsoas, rectus femoris, vastus medialis, vastus lateralis, adductor magnus, biceps femoris [2], semitendinosus, tibialis anterior, soleus, and gastrocnemius [2]), three ligaments (medial collateral ligament [MCL], lateral collateral ligament [LCL], and posterior cruciate ligament [PCL]) and two tendons (patellar and quadriceps). Knee ligament attachments were based on subject-specific anatomic landmarks obtained from the preoperative CT scans, and ligaments were modeled as nonlinear springs using previously published material properties [28]. The quadriceps and patellar tendons were modeled with contact-based rigid bodies to simulate contact and wrapping around the trochlear groove and tibial insert, respectively (Fig. 3).

Computer Simulation of Squatting

The computer-generated image of the simulation and photograph for one of the subjects during the squatting activity is shown in Fig. 4. The simulation was carried out in two steps and has been previously described in detail [15]. In the first step, skin marker-based motion data were used to prescribe the trunk, hip, knee, and ankle kinematics for an inverse-dynamics computation. During this step, joint torques and changes in muscle lengths were recorded throughout the activity cycle. In the next step, forward dynamics was used to compute the

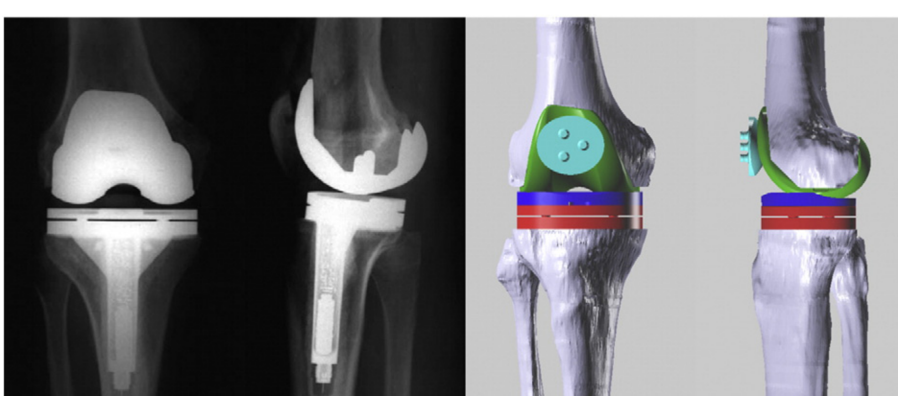

Fig. 2. Radiographs and corresponding CT-generated models of the implanted knee.

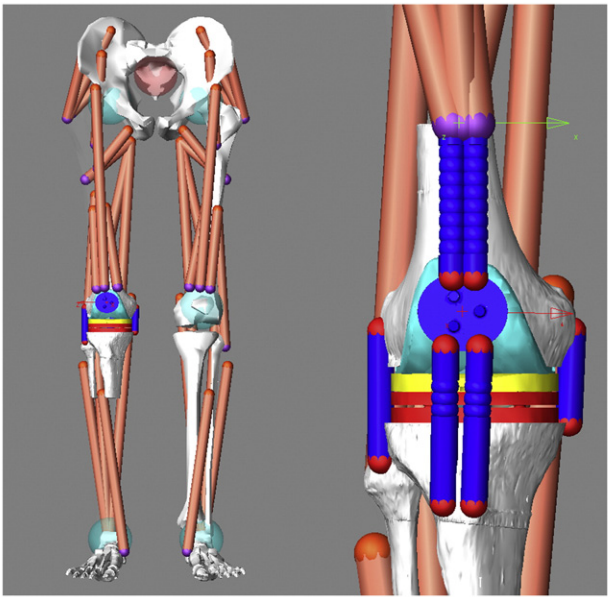

Fig. 3. Left: Lower extremity model constructed in LifeMOD; Right: Detail model of the implanted knee.

muscle forces required to reproduce the recorded changes in muscle lengths (to simulate muscle contraction). These muscle forces generated the required joint torque and force to reproduce the experimentally measured kinematics (used in the inverse-dynamics simulation). Tibiofemoral and patellofemoral contact forces during squatting were then computed from the forward dynamics analysis.

Results

Total ground reaction force was 0.9 to 1.1 × BW during squatting and was more or less evenly divided between extremities during squatting. Maximum passive flexion for was 100 and 110°, however, maximum flexion angle during squatting was only up to 92° to 96°. Peak forces measured during squatting were similar for both patients. Peak tibiofemoral contact forces in vivo were 2.4 × BW at 68°, 2.3 × BW at 71°, and 2.2 × BW at 74°, for the first patient; 2.4 × BW at 87°, 2.4 × BW at 86°, and 2.4 × BW at 90° for the second patient. However, the dynamic pattern of in vivo measured knee forces was different for both patients and also varied with the degree of trunk-flexion during squatting. While both patients squatted up to 90° flexion, contact forces peaked at different knee flexion angles. Our model predicted peak tibiofemoral contact forces of 2.2 to 2.3 × BW, which were close to those measured in vivo for each of the subjects (Fig. 5). When squatting with patient-preferred trunk flexion, deeper knee flexion was possible. Contact force peaked at 60° knee flexion and decreased with increasing trunk flexion after 60° knee flexion. In contrast, when squatting with minimal trunk flexion, patients were unable to squat beyond 60° knee flexion, and contact forces peaked at the maximum flexion angle. Model-predicted peak patellofemoral contact forces were 0.8 and 1.1 × BW for each patient respectively. Quadriceps forces peaked between

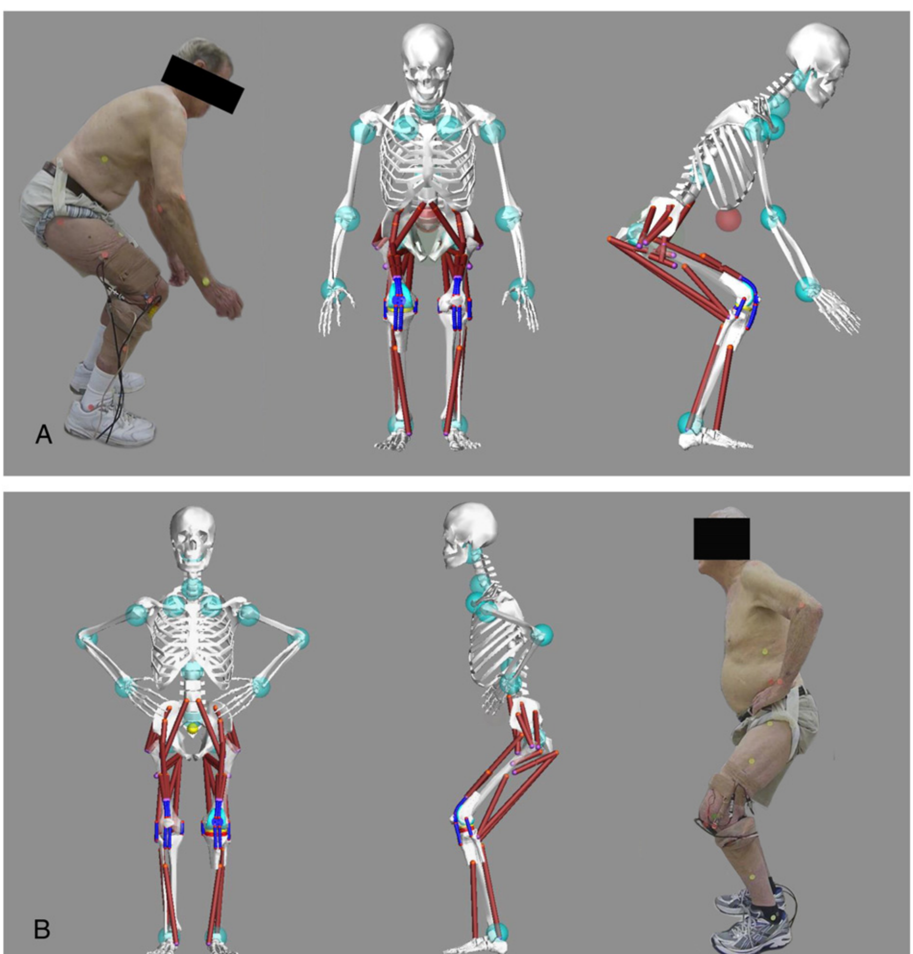

Fig. 4. (A) Photograph and corresponding model of patient squatting with patient-preferred trunk flexion. (B) Photograph and corresponding model of patient squatting with minimal trunk flexion.

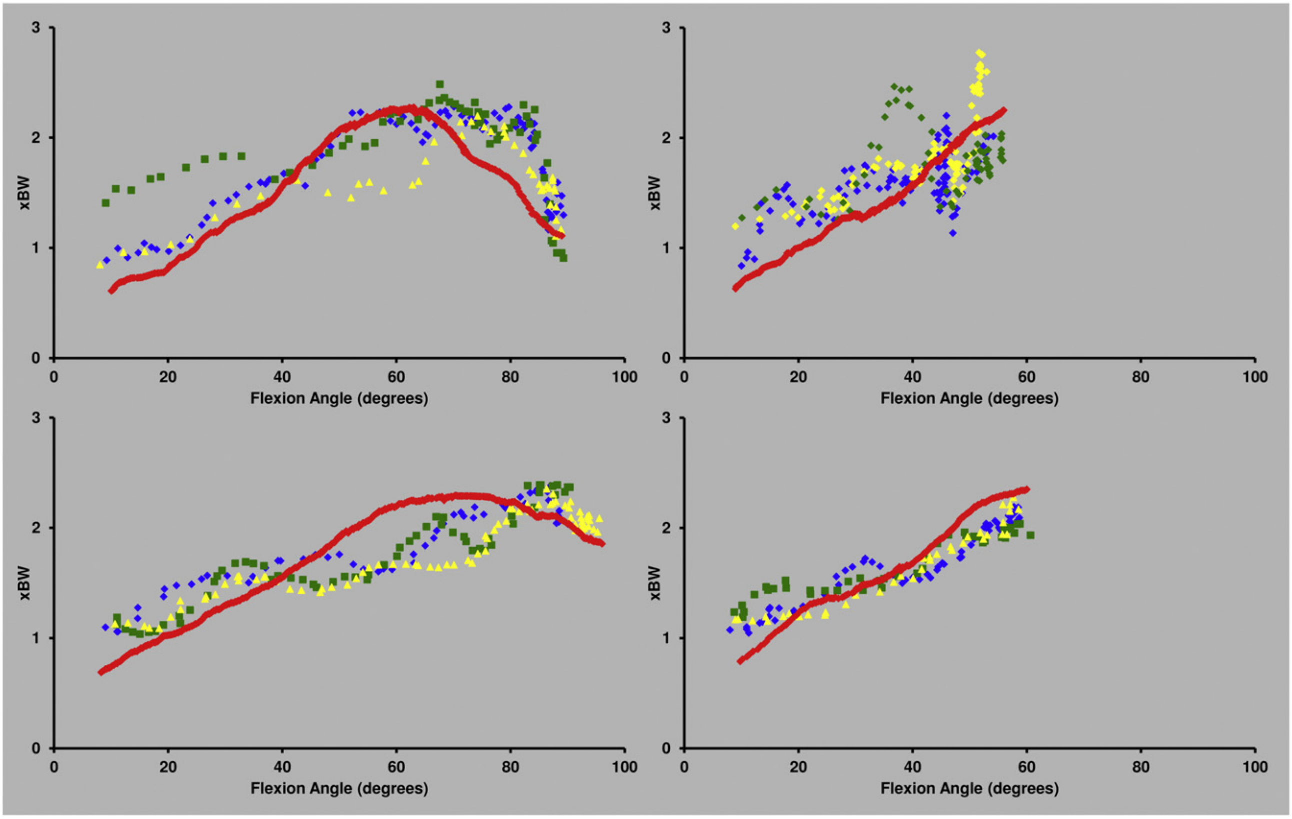

Fig. 5. Predicted tibiofemoral contact force magnitudes (bold red curve) compared to force measured over three cycles of squatting (green, yellow, and blue markers). Upper row: Patient 1; Bottom row: Patient 2; Left: Squatting with patient-preferred trunk flexion; Right: Squatting with minimal trunk flexion.

1.8 and 2.0 × BW, which also coincided with maximum tibiofemoral contact force.

Discussion

The contact force between components is one of the major factors influencing polyethylene wear and aseptic loosening. There are many reports of computer models predicting contact forces during various activities; however, there is a wide variation in contact forces predicted by computer models, even for similar activities such as walking [6–9] and squatting [11–14]. With the availability of knee forces measured in vivo, significant advances have been made in modeling, which have increased the accuracy of predicted forces during walking [23]. However, only one subject-specific model of squatting has been reported [15]. We therefore developed and validated two additional different patient-specific models that accurately predicted the femorotibial contact force based on in vivo measured tibial contact forces.

Peak tibiofemoral contact forces (2.2–2.3 × BW) were generally lower than those previously reported by other computer models [11–13,29–31]. For example, Smith et al computed peak forces averaging at 2.8 × BW and 3.8 × BW (peaking at average 125° and 139°) for different types of squatting in subjects without arthritis or TKA [13]. Shelburne et al predicted tibiofemoral contact forces peaking at 4.2 × BW at less than 90° knee flexion [12], while Nagura et al predicted tibiofemoral contact forces of 7.3 × BW, peaking at an average of 146° [30]. These differences in previous reports of computer models and our results may be in part due to differences in age (our subjects were older), due to surgery (post-TKA), and due to limited flexion (our subjects only flexed up to 90° during active squatting). The previously reported subject-specific model of squatting by Stylianou et al reported peak forces approximating 3.25 × BW. Stylianou et al modeled a 67-year-old female, weighing 78.4 kg. Our patients were males, older (by 16–21 years), and weighed less (69.5 and 76.3 kg). These subject-specific differences in knee forces that were accurately reflected in subject-specific models support the value of our modeling approach. These results also suggest that in the older post-TKA patient population, knee forces may be limited by the lower muscle strength.

In addition to differences in subject populations, there has been a general tendency for mathematical models of the knee to overestimate knee contact forces. Previous predictions for squatting have ranged from 2.8 × BW to 7.3 × BW [11–13,29–31]. Presumably, this overestimation is due to error in muscle moment arm measurement and due to assumptions used to predict antagonistic co-contraction. Smith et al reported that tibiofemoral contact forces were most sensitive to the estimate for quadriceps moment arm [13]. In our model, muscle moment arms were generated from CT-measured anatomic landmarks and our model predicted very little hamstring co-contraction. The predicted contact forces over the entire squatting cycle followed the pattern of experimentally collected in vivo data over multiple cycles with less than 10% difference. Moreover, differences in femorotibial contact force between the computer model and in vivo data were smaller than the experimental cycle-to-cycle variation within subjects.

Trunk flexion significantly affected tibiofemoral contact force, especially at higher knee flexion angles. Trunk flexion reduced the external flexion moment at the knee leading to reduced quadriceps force and therefore reduced tibiofemoral contact force. During walking, trunk flexion has also been shown to compensate for “quadriceps avoidance” gait during the stance phase [32]. Decreased contribution of the vasti muscles to vertical acceleration was associated with increased contribution of the contralateral back extensor muscle (erector spinae) and contralateral back rotators (internal and external obliques). Our model was able to accurately predict this effect of trunk flexion on contact force during squatting.

Peak patellofemoral contact forces and quadriceps muscle forces were also lower than previously reported [33]. Although others have reported on hamstring muscle activity during the squat, hamstring forces were low in our models in qualitative agreement with the EMG data.

EMG activity of hamstring muscles during the squatting activity is typically low and only necessary to prevent excessive hip flexion and to stabilize the knee [12,32,34–36]. The lack of significant hamstring antagonistic co-contraction reduces the total quadriceps force required to extend the knee and may also explain the lower tibiofemoral and patellofemoral contact forces.

One weakness of our model was that the software program did not use optimization of the muscle forces to reduce muscle redundancy and antagonistic co-contraction but used the muscle lengths calculated during the inverse dynamics phase to compute the required muscle forces during the forward dynamics phase. Another weakness was that although ligament attachment locations were based on subject-specific CT-generated bony landmarks the soft-tissue material properties were not subject-specific but were obtained from published averages. A third weakness, was that the peak passive flexion angle was 100° to 110°, however this was close to the mean reported for total knee arthroplasty in western populations [37]. Despite these limitations, the model predicted tibiofemoral contact force with reasonable accuracy in two different subjects performing two different squatting activities.

This model can be a very useful tool to predict the effect of surgical techniques and component alignment on contact forces. In addition, this model could be used for implant design development, to enhance knee function, and to predict forces generated during other activities. Finally, subject-specific models could be useful for predicting clinical outcomes.

Acknowledgments

In support of their research two of the authors (DD, BF) received, in any one year, outside funding in excess of $10,000 from the National Institutes of Health (R01 EB009351). None of the authors or their immediate families received payments or benefits to fund this research from a commercial entity, foundation, or any other source.

References

1. Rodricks DJ, Patil S, Pulido P, et al. Press-fit condylar design total knee arthroplasty. Fourteen to seventeen-year follow-up. J Bone Joint Surg Am 2007;89(1):89.
2. Vessely MB, Whaley AL, Harmsen WS, et al. The Chitranjan Ranawat Award: long-term survivorship and failure modes of 1000 cemented condylar total knee arthroplasties. Clin Orthop Relat Res 2006;452:28.
3. Devers BN, Conditt MA, Jamieson ML, et al. Does greater knee flexion increase patient function and satisfaction after total knee arthroplasty? J Arthroplasty 2011;26(2):178.
4. Noble PC, Gordon MJ, Weiss JM, et al. Does total knee replacement restore normal knee function? Clin Orthop Relat Res 2005;431:157.
5. D'Lima DD, Patil S, Steklov N, et al. The Chitranjan Ranawat Award: in vivo knee forces after total knee arthroplasty. Clin Orthop Relat Res 2005;440:45.
6. Lin YC, Walter JP, Banks SA, et al. Simultaneous prediction of muscle and contact forces in the knee during gait. J Biomech 2010;43(5):945.
7. Mikosz RP, Andriacchi TP, Andersson GB. Model analysis of factors influencing the prediction of muscle forces at the knee. J Orthop Res 1988;6(2):205.
8. Winby CR, Lloyd DG, Besier TF, et al. Muscle and external load contribution to knee joint contact loads during normal gait. J Biomech 2009;42(14):2294.
9. Taylor WR, Heller MO, Bergmann G, et al. Tibio-femoral loading during human gait and stair climbing. J Orthop Res 2004;22(3):625.
10. Fregly BJ, Besier TF, Lloyd DG, et al. Grand challenge competition to predict in vivo knee loads. J Orthop Res 2012;30(4):503.
11. Wilk KE, Escamilla RF, Fleisig GS, et al. A comparison of tibiofemoral joint forces and electromyographic activity during open and closed kinetic chain exercises. Am J Sports Med 1996;24(4):518.
12. Shelburne KB, Pandy MG. A dynamic model of the knee and lower limb for simulating rising movements. Comput Methods Biomech Biomed Engin 2002;5(2):149.
13. Smith SM, Cockburn RA, Hemmerich A, et al. Tibiofemoral joint contact forces and knee kinematics during squatting. Gait Posture 2008;27(3):376.
14. Lutz GE, Palmitier RA, An KN, et al. Comparison of tibiofemoral joint forces during open-kinetic-chain and closed-kinetic-chain exercises. J Bone Joint Surg Am 1993;75(5):732.
15. Stylianou AP, Guess TM, Kia M. Multibody muscle driven model of an instrumented prosthetic knee during squat and toe rise motions. J Biomech Eng 2013;135(4):041008.
16. D'Lima DD, Patil S, Steklov N, et al. Tibial forces measured in vivo after total knee arthroplasty. J Arthroplasty 2006;21(2):255.
17. D'Lima DD, Townsend CP, Arms SW, et al. An implantable telemetry device to measure intra-articular tibial forces. J Biomech 2005;38(2):299.
18. D'Lima DD, Patil S, Steklov N, et al. In vivo knee moments and shear after total knee arthroplasty. J Biomech 2007;40:S11.
19. D'Lima DD, Steklov N, Patil S, et al. The Mark Coventry Award: in vivo knee forces during recreation and exercise after knee arthroplasty. Clin Orthop Relat Res 2008;466(11):2605.
20. Varadarajan KM, Moynihan AL, D'Lima D, et al. In vivo contact kinematics and contact forces of the knee after total knee arthroplasty during dynamic weight-bearing activities. J Biomech 2008;41(10):2159.
21. D'Lima DD, Fregly BJ, Patil S, et al. Knee joint forces: prediction, measurement, and significance. Proc Inst Mech Eng H 2012;226(2):95.
22. D'Lima DD, Patil S, Steklov N, et al. The 2011 ABJS Nicolas Andry Award: 'Lab'-in-a-knee: in vivo knee forces, kinematics, and contact analysis. Clin Orthop Relat Res 2011;469(10):2953.
23. Kinney AL, Besier TF, D'Lima DD, et al. Update on grand challenge competition to predict in vivo knee loads. J Biomech Eng 2013;135(2):021012.
24. Kirking B, Krevolin J, Townsend C, et al. A multiaxial force-sensing implantable tibial prosthesis. J Biomech 2006;39(9):1744.
25. Mizu-Uchi H, Colwell Jr CW, Fukagawa S, et al. The importance of bony impingement in restricting flexion after total knee arthroplasty: computer simulation model with clinical correlation. J Arthroplasty 2012;27(9):1710.
26. Colwell Jr CW, Chen PC, D'Lima D. Extensor malalignment arising from femoral component malrotation in knee arthroplasty: effect of rotating-bearing. Clin Biomech (Bristol, Avon) 2011;26(1):52.
27. Weight, volume, and center of mass of segments of the human body. AMRL technical report. Wright-Patterson Air Force Base: United States Department of Commerce; 1969. p. 69.
28. Fishkin Z, Miller D, Ritter C, et al. Changes in human knee ligament stiffness secondary to osteoarthritis. J Orthop Res 2002;20(2):204.
29. Escamilla RF, Fleisig GS, Zheng N, et al. Biomechanics of the knee during closed kinetic chain and open kinetic chain exercises. Med Sci Sports Exerc 1998;30(4):556.
30. Nagura T, Matsumoto H, Kiriyama Y, et al. Tibiofemoral joint contact force in deep knee flexion and its consideration in knee osteoarthritis and joint replacement. J Appl Biomech 2006;22(4):305.
31. Dahlkvist NJ, Mayo P, Seedhom BB. Forces during squatting and rising from a deep squat. Eng Med 1982;11(2):69.
32. Li K, Ackland DC, McClelland JA, et al. Trunk muscle action compensates for reduced quadriceps force during walking after total knee arthroplasty. Gait Posture 2013;38(1):79.
33. Sharma A, Leszko F, Komistek RD, et al. In vivo patellofemoral forces in high flexion total knee arthroplasty. J Biomech 2008;41(3):642.
34. Dionisio VC, Almeida GL, Duarte M, et al. Kinematic, kinetic and EMG patterns during downward squatting. J Electromyogr Kinesiol 2008;18(1):134.
35. Ninos JC, Irrgang JJ, Burdett R, et al. Electromyographic analysis of the squat performed in self-selected lower extremity neutral rotation and 30 degrees of lower extremity turn-out from the self-selected neutral position. J Orthop Sports Phys Ther 1997;25(5):307.
36. Ohkoshi Y, Yasuda K, Kaneda K, et al. Biomechanical analysis of rehabilitation in the standing position. Am J Sports Med 1991;19(6):605.
37. Sumino T, Rubash HE, Li G. Does cruciate-retaining total knee arthroplasty enhance knee flexion in Western and East Asian patient populations? A meta-analysis. Knee 2013;20(6):376.